Petals, Tubes and Rings

The Structure of the Four-Direction Orbit

Fedge No

fedge-no@hotmail.com

Infinite Dimensional Wave Theory 11 November 2026

Abstract. The electron's orbit runs through four spatial directions. Its path has an exact closed form: the product of two turning directions, one turning once while the other turns L times. In one plane of view that path is a rose of petals, in another it is a set of nested rings, and along a third it is a tube. These are views of a single object. For every whole number L from 2 to 8 the orbit is linearly stable: it has no growing mode. Its petal tips are the vertices of a regular polygon inscribed in a circle, and its crossings of the axis in the end-on view lie exactly at the heights of those vertices, which is the construction chemists know as the Frost circle. Under the proton's own force the electron has stable orbits that fill a hollow tube; time averaged, the end of the tube shows a bright band or interior rings. There the ratio L is set by the radius, by an exact formula, and at the width that places Lyman-γ at one Bohr radius, the orbit of that radius has $L = 2.998$, very nearly three cycles through the fourth direction per revolution. The proton's down quark singles out that proton's fourth direction, which defines an orbit standing at a right angle to the petal orbit.

1. The path

Space has infinitely many ordinary spatial directions. The electron's orbit uses four of them. Call the coordinates x_1, x_2, x_3, x_4, and let θ advance steadily with time. At unit radius the orbit is

$$(x_1, x_2, x_3, x_4) = (\cos L\theta \cos\theta,\ \cos L\theta \sin\theta,\ \sin L\theta \cos\theta,\ \sin L\theta \sin\theta). \tag{1}$$

The sum of the four squares is one at every moment, so the electron never changes its distance from the centre. Everything that looks like a change of radius in a picture of this orbit comes from viewing four directions in two or three.

The structure is clearest with the four coordinates set out in a square array:

$$\begin{pmatrix} x_1 & x_2 \\ x_3 & x_4 \end{pmatrix} = \begin{pmatrix} \cos L\theta \\ \sin L\theta \end{pmatrix} \begin{pmatrix} \cos\theta & \sin\theta \end{pmatrix}. \tag{2}$$

The orbit is the product of two turning directions. One turns once per cycle and the other turns L times. This is what the orbit is. When L is a whole number the two turnings come back into step and the path closes.

2. The system that holds it

The path is an exact solution of a closed set of equations. The electron has position q and momentum p in six coordinates, and it is coupled to an antisymmetric 6×6 source C with

strength λ. The energy is

$$H = \tfrac{1}{2}|v|^2 - \frac{1}{|q|} + \tfrac{1}{4}\sum_{a,b} C_{ab}^2, \qquad v = p - \lambda C q, \tag{3}$$

and the equations of motion are

$$\dot q = v, \qquad \dot p = -\frac{q}{|q|^3} - \lambda C v, \qquad \dot C = \lambda\big[(Cq)\wedge v + q\wedge(Cv)\big], \tag{4}$$

where $a\wedge b = ab^{\mathsf T} - ba^{\mathsf T}$. Units are set by unit mass, unit attraction and unit source inertia, with $\lambda = 0.2$.

The orbit is a steady rotation $q(t) = \exp(\beta G_L t)\, q(0)$, with $\theta = \beta t$. The generator G_L rotates the (x_1, x_2) and (x_3, x_4) planes at rate 1 and the (x_1, x_3) and (x_2, x_4) planes at rate L. The source C is a 6×6 matrix over all six coordinates; the orbit uses four of them, and the other two stay at zero. Written out on the four active coordinates,

$$G_L = \begin{pmatrix} 0 & -1 & -L & 0 \\ 1 & 0 & 0 & -L \\ L & 0 & 0 & -1 \\ 0 & L & 1 & 0 \end{pmatrix}, \tag{5}$$

and $\dot x = \beta G_L x$ reproduces equation (1) at $\theta = \beta t$. The source rotates with the orbit, $\dot C = \beta[G_L, C]$. Take $q(0) = e_1$ and $p(0) = \beta G_L q(0) + \lambda C q(0)$. The orbit is steady when

$$\beta G_L\, p = -q - \lambda C v, \qquad \beta[G_L, C] = \lambda\big[(Cq)\wedge v + q\wedge(Cv)\big], \tag{6}$$

with $v = p - \lambda C q$ and $|q| = 1$. These are twenty-one equations, six for the momentum and fifteen for the source, in sixteen unknowns: the fifteen components of C and the rate β. They are consistent, and their solutions form a family for each L. A least-squares solve started from zero source, $C = 0$, and rate $\beta = 0.5$ reaches a residual below 2×10^{-10} and gives the rates and source sizes in Table 1. Direct integration of the full equations follows equation (1) to 5.2×10^{-10} and conserves energy to 2.1×10^{-11} at $L = 2, 3, 4, 5, 6$ and 8.

L	Rate β	Source size $\frac{1}{2}\sum C_{ab}^2$	Petals	Rings
2	0.455429	14.9537	4	2
3	0.299230	5.8240	3	2
4	0.223580	3.3347	8	4
5	0.169058	2.6546	5	3
6	0.148875	1.7187	12	6
7	0.127941	1.3855	7	4
8	0.112241	1.1721	16	8

Table 1. The locked orbits. Each row is the member of its family reached from $C = 0$, $\beta = 0.5$. Rings are counted outward from the centre.

Every one of these orbits is linearly stable. The linearized equations, including all fifteen source components, have no growing mode for $L = 2$ to 8: the largest real part of any eigenvalue falls in proportion to the numerical step, to 1.5×10^{-7} at the finer step. A push of size 10^{-4} integrated for ten full turns moves the radius by at most 1.4×10^{-4}. The case $L = 1$ is different: its path is an offset circle.

3. One path, many views

Equation (2) shows at once why the same orbit has such different pictures. Read along the top row and the path in the (x_1, x_2) plane is

$$x_1 + ix_2 = \cos(L\theta)\, e^{i\theta}, \tag{7}$$

a rose of petals. Read down the first column and the path in the (x_1, x_3) plane is

$$x_1 + ix_3 = \cos(\theta)\, e^{iL\theta}. \tag{8}$$

The two angles have traded places. The slow angle now sets the size and the fast angle winds around, so the curve goes round L times while its size changes slowly: a set of nested rings. Figure 1 turns the orbit from one view to the other. Nothing about the orbit changes between the panels.

The tube appears in a third choice of axes. Combining the rows of equation (2) gives two complex coordinates in two perpendicular planes,

$$u = \frac{(x_1 + ix_2) + i(x_3 + ix_4)}{\sqrt{2}} = \frac{e^{i(L+1)\theta}}{\sqrt{2}}, \qquad v = \frac{(x_1 + ix_2) - i(x_3 + ix_4)}{\sqrt{2}} = \frac{e^{-i(L-1)\theta}}{\sqrt{2}}. \tag{9}$$

In each of these planes the path is a plain circle of radius $1/\sqrt{2}$. Viewed in the plane $X + iY = \cos\chi\, v + \sin\chi\, u$, the radius seen end-on obeys

$$r^2 = \tfrac{1}{2}\big[1 + \sin(2\chi)\cos(2L\theta)\big]. \tag{10}$$

At $\chi = 0$ the radius is constant, and with one coordinate of the u plane as height the path lies on the wall of a cylinder. For $0 < \chi < 45^\circ$ the radius moves between two turning values and the end of the tube is an annulus. At $\chi = 45^\circ$ the inner radius reaches zero and the petals return (Figure 2). The full radius stays one throughout.

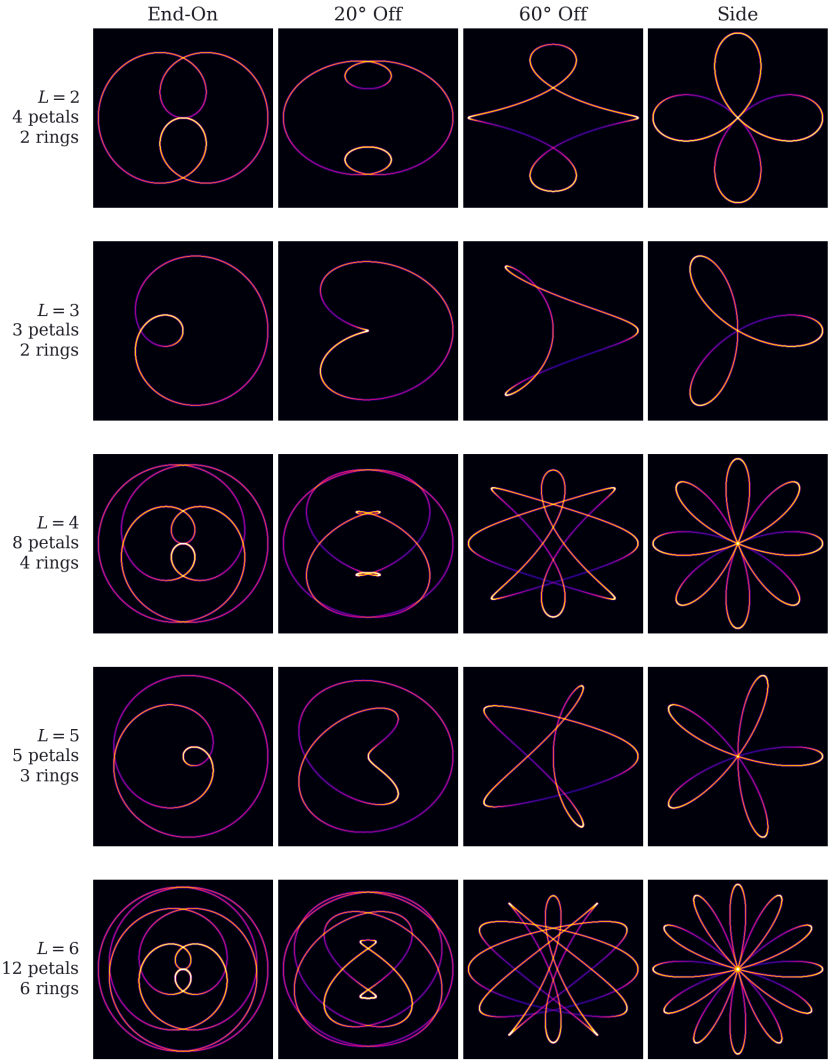


Figure 1. One locked orbit at five values of L, turned from the end-on rings of equation (8) to the side-on petals. Each panel is a time-averaged ironbow heat map of the exact path, with closer parts of the path brighter.

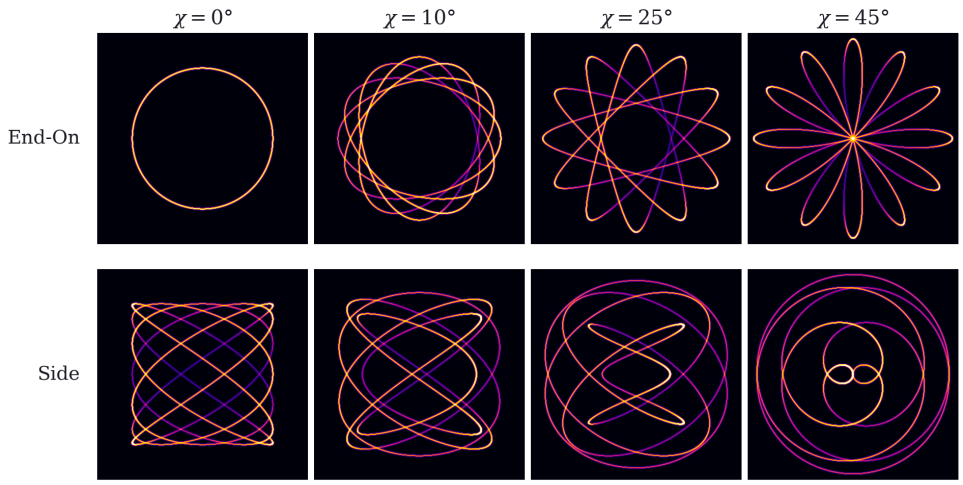


Figure 2. The $L = 6$ orbit viewed at four values of χ. At $\chi = 0$ it lies on a cylinder, at intermediate χ its wall thickens, and at $\chi = 45°$ it is the twelve-petal rose.

4. Counting petals and rings

Both counts follow directly from the path. The petal tips lie where $|\cos L\theta| = 1$, at $L\theta = \pi j$. There are $2L$ such moments in one turn. Advancing θ by π multiplies $\cos(L\theta)e^{i\theta}$ by $(-1)^{L+1}$, so for odd L the second half of the turn retraces the first. Even L therefore has $2L$ petals and odd L has L petals.

A ray from the centre at angle ϕ in the end-on view of equation (8) meets the curve where $L\theta = \phi + \pi j$, with the sign of $\cos\theta$ matching the parity of j. The ring count is the number of strands a ray in general position crosses, counted outward from the centre. For even L such a ray crosses exactly L strands. For odd L the curve closes in half a turn, and a ray crosses $(L+1)/2$ or $(L-1)/2$ strands depending on its direction. Counted outward from the centre, even L has L rings and odd L has $(L+1)/2$. Along the x_1 axis the strands cross at the radii $|\cos(\pi k/L)|$, confirmed by direct integration at $L = 3, 4, 5, 6$ and 8, and at $L = 2$ for the outer crossing; the $L = 2$ crossing at the centre is a tangency. For odd L the path also passes through the centre where $\cos\theta = 0$, which is not one of these crossings.

5. The regular polygon

For a ring of N atoms, the energy levels of its π electrons in Hückel's theory [1] are

$$E_k = \alpha + 2\beta\cos\frac{2\pi k}{N}, \qquad k = 0, \ldots, N-1. \tag{11}$$

Frost and Musulin [2] showed that these levels can be read from a picture: inscribe a regular N-gon in a circle with one vertex at the bottom, and the heights of the vertices are the levels. The orbit reproduces this construction exactly.

Take the petal tips, at $L\theta = \pi j$. Each lies on the unit circle at $(-1)^j e^{i\pi j/L}$. These points are the vertices of a regular N-gon, with $N = L$ for odd L and $N = 2L$ for even L. Their x_1 coordinate is

$$x_1 = (-1)^j\cos\frac{\pi j}{L} = \cos\frac{\pi j(L+1)}{L}. \tag{12}$$

For odd L this is $\cos(2\pi jm/L)$ with $m = (L+1)/2$, and m shares no factor with L. For even L it is $\cos(2\pi j(L+1)/2L)$, and $L+1$ shares no factor with $2L$. In both cases j runs through every level $\cos(2\pi k/N)$ with its full degeneracy. The heights of the polygon's vertices are the levels.

The moments $L\theta = \pi j$ are also the moments when the end-on view of equation (8) crosses its axis, and x_1 is shared between the two views. The orbit therefore performs Frost's projection by itself: the end-on rings cross the axis at the heights of the vertices of the polygon formed by the petal tips (Figure 3). Table 2 lists the levels.

The tip counts have a sharp arithmetic. A locked orbit has either an odd number of tips or a multiple of four. It never has $4n + 2$ tips: no locked orbit has 6, 10 or 14. Those are exactly the ring sizes of Hückel's aromatic rule, which counts $4n + 2$ π electrons; in a neutral C_NH_N ring the count equals the ring size. The radii of the $L = 3$ orbit are 1 and $\frac{1}{2}$, the sizes of benzene's levels $\pm 2\beta$ and $\pm\beta$, while its signed crossings form the triangle.

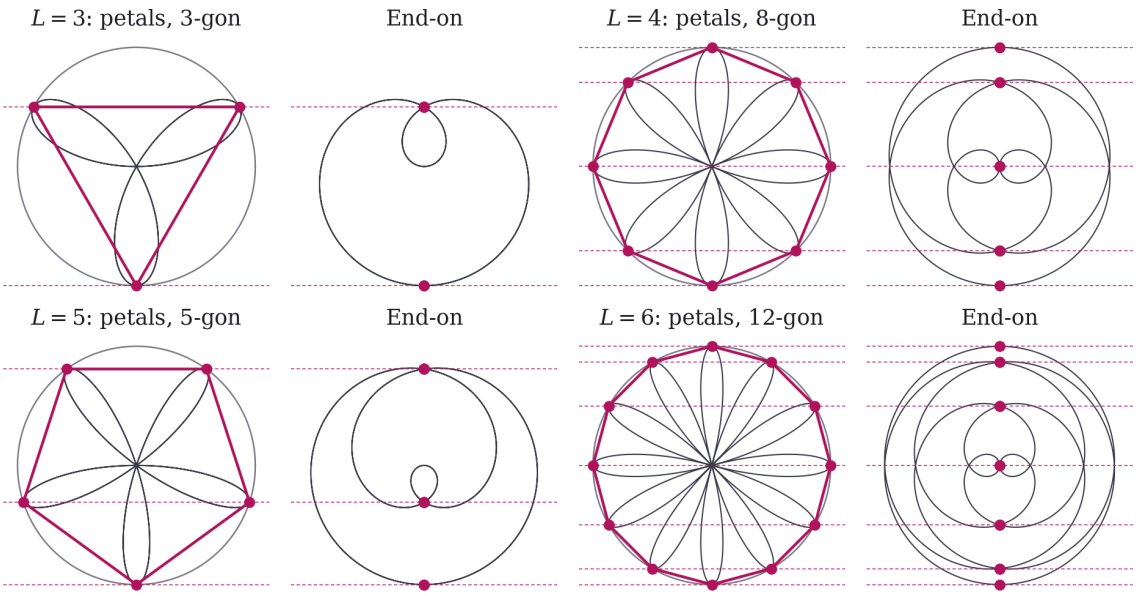


Figure 3. Petal tips form a regular polygon inscribed in the circle, drawn vertex down as in Frost's construction. Dashed lines carry the vertex heights across to the end-on view, where the orbit crosses its axis at those same heights. The path also passes through the centre whenever $\cos\theta = 0$; for odd L that passage is not one of the marked crossings.

L	N	Levels $\cos(2\pi k/N)$, with degeneracy
3	3	$1,\ -\frac{1}{2}\ (\times 2)$
4	8	$1,\ 0.707\ (\times 2),\ 0\ (\times 2),\ -0.707\ (\times 2),\ -1$
5	5	$1,\ 0.309\ (\times 2),\ -0.809\ (\times 2)$
6	12	$1,\ 0.866\ (\times 2),\ 0.5\ (\times 2),\ 0\ (\times 2),\ -0.5\ (\times 2),\ -0.866\ (\times 2),\ -1$

Table 2. The signed axis crossings over one closed cycle. For $L = 6$ the list has twelve levels in all, once each around the 12-gon.

6. Tube orbits under the proton's force

The proton's force on the electron has two parts, in atomic units:

$$V = -\frac{4/3}{\sqrt{x^2 + y^2 + z^2 + w^2 + R_u^2}} + \frac{1/3}{\sqrt{x^2 + y^2 + z^2 + R_d^2}}, \tag{13}$$

The two up quarks pull through the four-direction distance. The down quark pushes through the three-direction distance. The softenings $R_u = 0.01524\,s$ and $R_d = 0.00653\,s$ are set by the single width parameter s. Because the push has no dependence on w, the force is symmetric about the w axis and w is the axis of the tube.

The motion runs in (x, y, w) with $z = 0$. The electron starts at $(r, 0, 0)$ with velocity $f\,v_c\,(0, \cos\alpha, \sin\alpha)$, where $v_c = \sqrt{g\,r}$ is the circular speed set by the net inward pull g at the launch point (up pull less down push), f is the speed fraction and α is the tilt out of the plane $w = 0$. One revolution is $T_0 = 2\pi r/v_c$. Integration is by the fourth-order symplectic Yoshida

method at 1000 steps per revolution. A twin orbit starts 10^{-7} away in x, and its separation after the run, divided by 10^{-7}, is the growth factor. The inner and outer radii are the least and greatest $\sqrt{x^2 + y^2}$, and the half-length is the greatest $|w|$.

The grid is three widths ($s = 100, 90, 0.49$), four launch radii (0.5, 1, 2, 4), four speed fractions (0.6, 0.8, 1, 1.2) and eight tilts (10°, 30°, 50°, 70°, 80°, 85°, 88°, 89.5°), 384 launch conditions. At $r = 0.5$ with $s = 100$ and 90 there is no inward pull, which leaves 320. Of these 320 orbits, 242 are stable over 300 revolutions: energy drift below 10^{-6} and growth factor below 10^4. Of those, 217 are hollow tubes, with inner radius and half-length both more than a tenth of the outer radius.

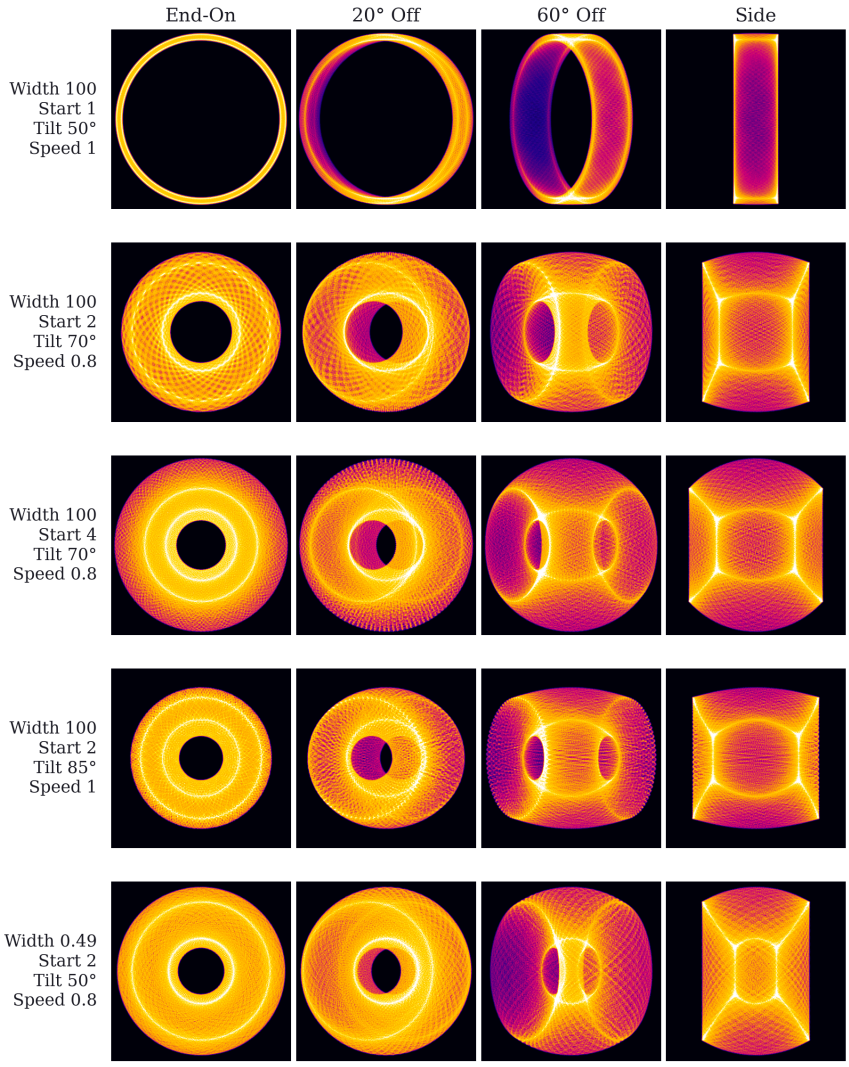


Figure 4. Stable orbits under the proton's force, time averaged over 2000 revolutions and shown in ironbow, closer parts brighter. End-on, each tube shows its hollow centre. The first orbit's end is a single thin band, the second shows one bright inner ring, and the other three show two rings each. Turning the view shows the rings as the ends of bright bands running along the tube.

Figure 4 shows five of them, the rows $(s, r, \alpha, f) = (100, 1, 50°, 1)$, $(100, 2, 70°, 0.8)$,

Width s	Start r	Tilt	Speed	Inner radius	Outer radius	Half-length	Energy drift
100	1	50°	1	0.9212	1.0000	0.2586	1.3×10^{-10}
100	2	50°	1	1.4597	2.0000	1.2371	8.1×10^{-11}
100	2	70°	0.8	0.7759	2.0000	1.3367	1.3×10^{-9}
100	4	70°	0.8	1.1528	4.0000	3.0876	1.2×10^{-8}
100	1	85°	1	0.8534	1.0000	0.3388	3.9×10^{-10}
100	2	85°	1	0.6293	2.0000	1.7888	2.1×10^{-9}
90	2	88°	1	0.4502	2.0000	1.8831	3.9×10^{-9}
0.49	2	50°	0.8	0.5579	2.0000	1.2765	1.0×10^{-7}

Table 3. Eight tube orbits integrated for 2000 revolutions. Halving the integration step cut the energy drift sixteen-fold, to the values shown, and left the radii and lengths unchanged to within 2×10^{-6} at $s = 100$ and 90 and to within 2.4×10^{-5} at $s = 0.49$. Radii and lengths are in Bohr radii.

$(100, 4, 70°, 0.8)$, $(100, 2, 85°, 1)$ and $(0.49, 2, 50°, 0.8)$. These orbits do not close in general, so over time the path fills the tube, and the time average shows a bright hollow-centred end, with interior rings in the wider tubes.

The law gives the ratio L directly. For a nearly circular orbit of radius r in the plane $w = 0$, the fourth-direction motion has squared rate $(4/3)(r^2 + R_u^2)^{-3/2}$, the pull of the up quarks alone, while the revolution has squared rate equal to the net pull per unit radius, which includes the down quark's push. Their ratio is

$$L^2 = \left[1 - \frac{1}{4} \left(\frac{r^2 + R_u^2}{r^2 + R_d^2} \right)^{3/2} \right]^{-1} . \tag{14}$$

Far from the proton $L = \sqrt{4/3} = 1.1547$. Moving inward, L rises steadily and grows without limit at the inner edge where the net pull vanishes. Every whole number from 2 upward therefore occurs at exactly one radius. Table 4 gives those radii at width 100, the width that places the line Lyman-γ at one Bohr radius [3]. The radii scale in proportion to s. At width 100 the orbit at one Bohr radius has $L = 2.998$: the electron moves through the fourth direction very nearly three times per revolution.

Whole-number ratio L	2	3	4	5	6	inner edge
Radius at $s = 100$	1.1529	0.9999	0.9565	0.9377	0.9279	0.9062
Measured ratio	2.0000	3.0001	4.0001	5.0002	6.0002	

Table 4. Radii at which equation (14) gives a whole number, and the ratio measured by direct integration at a tilt of 0.5°.

7. Orientation

The up quarks' pull depends on the four-direction distance, which has no preferred direction. To an up quark the four directions are interchangeable. The down quark's push depends on the three-direction distance, and in doing so it singles out one direction: that proton's fourth direction.

Two orbits follow. In the petal orbit the basic revolution lies in the observed directions and the precession carries it through the fourth. In the *orthogonal* orbit the fourth direction takes part in the basic revolution and an observed direction carries the precession. The basic orbit stands at a right angle to the petal orbit, measured against the proton's fourth direction. The tilts of 85° and 88° in Table 3, at which the launch velocity lies almost wholly in the fourth direction, are orbits of this kind.

8. Where these results hold

In the locked system the whole number L is carried by the source, and the equations of Section 2 hold for each value. Under the proton's force, equation (14) sets L continuously from the radius, and each whole number occurs at one radius.

The locked orbits are stable in their linear spectrum and in ten-turn integrations. The tube orbits are stable over the stated numbers of revolutions.

All results here are for one electron around one nucleus.

References

[1] E. Hückel, Quantentheoretische Beiträge zum Benzolproblem I, *Z. Phys.* **70**, 204 (1931).

[2] A. A. Frost and B. Musulin, A mnemonic device for molecular orbital energies, *J. Chem. Phys.* **21**, 572 (1953).

[3] F. No, The Four-Direction Orbit: Width, Tilt, Molecules and the Hidden Rotation (2026).